ALLOY CARBIDE PRECIPITATION IN A HIGH COBALT-NICKEL SECONDARY HARDENING STEEL

J. Liddle, G. Smith, G. Olson

JOURNAL DE PHYSIQUE
Colloque C7, supplément au n° 11, Tome 47, Novembre 1986 C7-223

ALLOY CARBIDE PRECIPITATION IN A HIGH COBALT-NICKEL SECONDARY HARDENING STEEL

J.A. LIDDLE, G.D.W. SMITH and G.B. OLSON

Department of Metallurgy and Science of Materials, University of Oxford, Parks Road, GB-Oxford OX1 3PH, Great-Britain
Department of Materials Science and Engineering, Massachusetts Institute of Technology, Cambridge, MA 02139, U.S.A.

Abstract - The process of alloy carbide precipitation in a high cobalt-nickel secondary hardening steel, AF1410 (Fe - 14 wt%Co - 10%Ni - 2%Cr - 1%Mo - 0.16%C) has been studied by FIM and atom probe techniques. The evolution of the alloy carbides has been followed in detail for the standard heat treatment temperature of 510°C. The first evidence of brightly-imaging solute clusters is observed after an ageing time of 1 minute, and the first traces of a rod-like morphology emerge after 30 minutes. Very slow growth of the rod-like carbides takes place between 30 minutes and 5 hours ageing, accompanied by a slow decrease in hardness. This is followed by rapid coarsening and spheroidisation, during which a marked loss of hardness occurs. The size and composition variation of the carbides has been followed throughout the ageing treatment. A model for the growth and coarsening of the particles is presented.

1 - INTRODUCTION

High Co-Ni secondary hardening steels exhibit outstanding combinations of strength and toughness. The HP94X steels were the first of this type. These were followed by HY180 [1] and then by AF1410 [2]. The latter exhibits the best combination of strength and toughness of any commercially available steel. It is therefore important to discover the reasons for its outstanding properties.

A preliminary FIM/AP investigation by Chang et al. [3] looked at material in the standard heat treated and overaged conditions, and revealed the presence of small rod-like carbide particles. A TEM examination of heavily overaged material, by Krzanowski (unpublished) showed the presence of much coarser carbides. The present work is intended to provide a more systematic study of the growth of these alloy carbides at the standard heat treatment temperature.

2 - MATERIALS AND EXPERIMENTAL TECHNIQUES

The material examined was supplied by Carpenter Steel Co., Reading, Pennsylvania, U.S.A. Four pieces 12.5mm square and 100mm long were cut from an ingot of composition .163C, 1.03Mo, 2.10Cr, 10.21Ni, and 14.24Co (wt%) bal. Fe. The initial heat treatment used on these samples was 1.5hrs at 830°C; oil quench; 1 hr at -70°C; air warm. With an ageing treatment of 5hrs at 510°C this material gave K_{IC} values of 200MPa $m^{1/2}$ and U.T.S. values of 1.65GPa. Material for examination in the TEM and FIM was tempered in the form of small sheets (0.5mm x 5mm x 35mm). For times up to 15 mins samples were treated in a salt bath, while

for longer times samples were furnace-treated after sealing into silica tubes under .25 atmosphere of Ar, in order to prevent decarburization and oxidation. All tempering was carried out at 510°C, and samples were quenched into iced water.

Optical microscope, SEM, TEM, FIM and atom probe examination of the samples was carried out. Both the older Oxford FIM/AP with a 125cm straight flight tube, and the newer FIM 100 with a 226cm curved flight tube with a Poschenrieder type energy compensator were used in this work. These instruments have been described in detail elsewhere [4] [5]. FIM specimens were prepared by a standard two stage electropolishing technique; the first stage using a 25% perchloric acid 75% acetic acid electrolyte, and the second stage 2% perchloric acid in 2-butoxyethanol.

3 - RESULTS

Hardness Measurements

Hardness values against ageing time at 510°C were obtained for total ageing times of up to 16hrs (See Fig.1). As can be seen the hardness of the as received material is high, at 530HV. On tempering there is a rapid initial increase in hardness, followed by a slower rise to a peak hardness of 574HV after 15 mins. The hardness falls slowly until 5hrs, and then declines sharply between 5 and 16hrs - suggestive of either a recovery process coming into play, or the onset of rapid coarsening, or both.

FIM

FIM pictures of AF1410 were taken in the as received condition, and after ageing at 510°C for 1, 5, 15, and 30mins and 1, 3, 5, 8 and 16hrs (see Fig.2). The photographs show typical structures seen at the various ageing times. In the as received condition the most noticeable features are the small randomly distributed brightly imaging spots, believed to be Mo atoms. After tempering for 1 and 5mins small clusters of bright atoms appear - the size of which is very difficult to estimate accurately because of the extra magnification of protrusions [6] [7]. At 15mins (the time associated with peak hardness) larger clusters are seen. After tempering for 30mins the first indications of a rod like morphology are apparent. As time proceeds the shape of the particles becomes more clearly defined, and the size increases slightly. The micrographs show the particles in various orientations; when the rods intersect the surface at right angles they display a roughly circular or hexagonal cross-section. At longer ageing times (i.e. 8 and 16hrs) there is a very marked change in morphology from rods to spheroids, and rapid coarsening of the particles takes place.

Comparison with the graph of hardness vs ageing time shows that the initial cluster formation corresponds to the rise to peak hardness, while the development of the rod-like morphology up to tempering times of 5hrs is associated with a relatively small decrease in hardness, and the spheroidisation and coarsening corresponds to the rapid fall in hardness between 5 and 16hrs.

It has been assumed that the alloy carbides in such steels are nucleated on dislocations. It is sometimes possible to see if this is the case using the FIM, because when dislocations intersect a prominent pole the concentric rings round the pole will be converted into spirals if the dislocations have a Burgers vector component normal to the surface. However, it is not particularly easy to observe this because brightly imaging atoms tend to draw imaging gas from the surrounding area and so render the relevant region of matrix barely visible. Also dislocations do not always conveniently intersect prominent poles. Despite these difficulties however, particles were seen to lie on dislocations in some instances, but this is by no means always the case.

Particle number densities were obtained for all the heat treatments examined in the FIM (see Fig.3). This was done by counting the number of particles in a particular micrograph, dividing by the field of view, and dividing again by the average particle size; this last because, as the particles get larger each one has a greater chance of intersecting a given sampling plane. (The particle size was taken to be the average of the largest and smallest dimensions of a particular set of particles). It should be pointed out that there are several sources of error involved in such measurements. At short times, i.e. 1 and 5mins, it is very difficult to decide what is and is not a particle. This is not helped by the fact that as the field of view increases with increasing voltage, the particles appear smaller; and what may have passed as a cluster of atoms at a lower voltage now appears the same size as a single atom did previously. However, as the ageing times get longer, and the particles become more clearly defined, this ceases to be a problem. Unfortunately, though, the number of particles starts to fall rapidly, for ageing times of 1hr or more, and so the statistical error becomes more significant.

To give some idea of the weight that should be given to each point on the graph, the numbers of particles examined for each heat treatment were, on average, 170 for times of 1-30mins and 25 for times of 1-8hrs. All the points are plotted with error bars of one population deviation on either side. The line of best fit calculated from this graph for ageing times between 15mins and 16hrs has the equation:

$$\mathrm{Ln}(n/10^{22}) = -1.03 \times \mathrm{Ln}(t) + 3.59$$

i.e.

$$n \simeq 36 \times 10^{22}/t$$

where t is in hours.

The correlation coefficient calculated was 0.965, indicating a good fit to this line.

A graph of apparent particle size vs ageing time was obtained (Fig.4) by measuring the particle image sizes from the micrographs. (The largest dimension of each particle has been taken as its size). The additional magnification factor makes interpretation of the results difficult, since at small particle sizes the extra effect will be large, but as the particles approach the size of the tip their apparent size will tend towards their actual size. The change in morphology is also an important factor. However, it is still possible to make some general comments on the graph.

At the shortest ageing times the particle size appears to be roughly constant, but, as ageing continues there is a smooth increase in particle size, with a small discontinuity at 5hrs (particle size 120 Å). If a line of best fit is calculated for this graph, for times of 15mins onwards, its equation is:

$$\mathrm{Ln}(r) = 4.28 + 0.428 \times \mathrm{Ln}(t)$$

i.e.

$$r \simeq 72 \times t^{0.43}$$

where r is in Å, and t is in hrs.

The correlation coefficient calculated for this line is 0.987, which again indicates a good fit to the data.

Atom Probe Analysis

Atom probe analysis was carried out on all heat treatments examined by FIM. The compositions of the particles probed for each heat treatment are given below:

Heat treatment		Fe:Cr:Mo	M:C
1hr	75 ions	.94: 1:.53	7.6:1
	69 ions	.17: 1:.83	4.0:1
	116 ions	0.0: 1:2.0	7.5:1
3hrs	73 ions	2.9: 1:1.2	15.7:1
	67 ions	1.0: 1:1.3	11.5:1
5hrs	192 ions	0.0: 1:.47	4.4:1
8hrs	308 ions•	0.0: 1:0.5	3.0:1
	504 ions+	0.0: 1:.92	2.3:1
16hrs	150 ions+	0.0: 1:.75	2.2:1

(• = With image gas, + = Without image gas)

Since at the shorter ageing times the particles are relatively small, the probe hole covers part of the matrix, and so matrix material is analysed along with the particle. In order to obtain a more accurate composition, in these cases, it was assumed that of the elements Fe, Ni and Co, only Fe would actually be part of the carbide particle. To correct for the Fe analysed from the surrounding matrix the numbers of Co and Ni ions appearing in each particle analysis were added and the appropriate number of Fe ions $(\%Fe/(\%Co + \%Ni) = 3)$ were subtracted from the analysis.

As can be seen from these results, the quantity of carbon being analysed from each particle is well below what would be expected from M_2C carbides that are formed in Mo/Cr containing steels. It was suggested that the presence of image gas might somehow affect the amount of carbon detected. This same effect has been observed in the analysis of bainite [6]. To see if this was indeed the case, it was decided to probe two carbides in the 8hr aged sample; one with, the other without image gas present. As is evident from the table there is a significant difference between the two cases.

Despite the uncertainty of these results some interesting trends can be seen. At shorter ageing times it appears that there is a relatively high Fe content to the particles, but this falls to zero as the particles begin to coarsen rapidly. It is also clear that, even allowing for the possible effects of probing with image gas present, the compositions of the particles are not close to an M_2C stoichiometry. This is particularly pronounced for samples aged for short times. The composition tends towards M_2C as ageing proceeds. In addition, the Cr/Mo ratio varies as a function of ageing time; at short times the ratio is close to, or even less than 1, but this is reversed for longer times, as was shown by Chang et al. [3].

Random area analyses were also made of material heat treated for times of less than 1hr. In the samples aged for 1 and 5mins, the carbon was not evenly distributed in the material, because the amount picked up was a factor of two too low. This suggests that, at these ageing times the carbon is "locked up" in specific areas; perhaps in cementite particles. At ageing times of 15 and 30mins the carbon analyses are much closer to what would be expected from the bulk composition. This suggests that the carbon is now more evenly distributed in the material - which is consistent with the appearance of the first fine alloy carbides (i.e. the analysis integrates over many fine clusters).

Boundaries decorated with brightly imaging atoms were found in samples aged for 1, 5 and 8hrs. It proved possible to analyse the boundaries in the 1 and 8hr specimens. Segregation of Cr, Mo and C to the boundaries was observed. In both instances the problem of the probe hole covering the matrix as well as the area of interest was encountered, and quantitative estimation of segregation was difficult.

4 - DISCUSSION

The precipitation sequence occurring in AF1410 is complex, involving the transformation of alloy carbides from clusters to rods to spheroids and thence to larger rods, as shown schematically in Fig.5. It is interesting to compare this study with the work of Davies [9] and Davies and Ralph [10], who examined a 3.5Mo 0.2C steel. A comparison of the times and temperatures studied is given in the table below:

	AF1410			Fe-3.5Mo-0.2C	
Temp °C	510	593*	540	575	650
Time (s)					
10	solute atoms				
10^2	small clusters				
10^3	small rods			spheroids	spheroids
10^4	spheroids		spheroids		rods
10^5		rods		rods	
10^6			rods		

(*TEM by J.Krzanowski at AMRRC, Watertown, U.S.A.).

It is interesting to note the considerably slower kinetics of precipitate growth apparent in the 3.5Mo 0.2C alloy; a peak hardness of 574HV is reached in 15mins by AF1410 at 510°C while the model alloy takes 10hrs to reach peak hardness at 575°C. (A similar 4.0Mo 0.2C alloy examined by Irani et al. [11] gave a peak hardness of 400HV after 5hrs at 600°C). Unfortunately, it is not possible to compare the results obtained for AF1410 at short ageing times with ones from the 3.5Mo 0.2C alloy, since, perhaps surprisingly, no work was done on this alloy at short tempering times. The reason for the large difference in kinetics is thought to be due to the much finer dispersion of alloy carbides produced in AF1410, which results from the higher dislocation content, and the greater diffusivity of Cr compared to Mo. The dislocations will provide short circuit paths for diffusion of solute atoms to particles (especially dislocation nucleated ones), and the higher diffusivity of Cr will increase the flux of solute atoms for precipitate growth still further.

Once the levels of Cr, Mo and C have reached sufficiently high values in the clusters, coherent, rod-like precipitates start to form. As tempering continues, the rod-like particles in AF1410 grow until they reach a critical length of about 120 Å. At this point lengthening appears to cease and thickening takes place. The lattice constant of the ferrite matrix along $[100]$ is calculated as 2.872 Å and the lattice constant of M_2C along $[11\bar{2}0]$ is 2.96 Å as measured by Krzanowski from carbides extracted from overaged AF1410). The lattice mismatch is therefore predicted to reach one repeat distance i.e. 2.96 Å in a length of 33.6 unit cells, or about 100 Å. Given that the Fe content in carbides produced after short ageing times will probably reduce the mismatch between carbide and matrix further, and Cr is known to reduce the lattice parameter of M_2C carbides [12], then the observed

critical length of 120 Å is in good agreement with that calculated. For the precipitates to grow any further they must generate interface dislocations to accommodate the increasing mismatch. However, the Burgers vectors of these interface dislocations - which take the form of edge loops - are large. This means that they probably cannot be generated around particles less than about 40 Å in diameter. The rods thus reach a critical length, and then have to overcome a type of "activation barrier" and lose full coherency, to be able to grow any further, so they will tend to thicken rather than lengthen. This explains the discontinuity in the plot of particle size vs ageing time, and the sudden change in morphology. As the particles increase in size still further, it becomes possible for the necessary interface dislocations to be produced, which leads to another change in morphology back to rods. This time, however, the rods are coherent in lengths of ~120Å, separated by interface dislocations. There is now no obstacle to further growth, and the precipitates coarsen as expected.

The graph of apparent particle size vs ageing time gives r as proportional to $t^{0.43}$. However, as was mentioned earlier, the difference between actual and apparent particle sizes decreases as the particle sizes increase - which leads to the graph having a gradient closer to 0.5, i.e. r proportional to $t^{1/2}$. It is interesting to compare this result with that obtained for longer ageing times by Davies who found r proportional to $t^{1/3}$. We can see that the two time exponents obtained from the two sets of data correspond to interface control being the mechanism operating in AF1410, at the times studied, and to lattice diffusion being the controlling factor in the coarsening of the precipitates under the ageing conditions studied by Davies. This result may be explained if it is assumed that interface control occurs when the particles are coherent and that diffusion control operates when coherency breaks down.

Acknowledgements

This work was supported by the United States Army Research Development and Standardisation Group under contract No.DAJA45-86-M-0187.

References

[1] Speich G.R., Dabkowski D.S. and Porter L.F., Met. Trans. 4 (1973) 303.

[2] General Dynamics, U.S.Patent, No. 4,076,525. (1978).

[3] Chang L., Smith G.D.W. and Olson G.B., J. De Physique Supplement to No.3 47 (1986) 265.

[4] Cerezo A., Smith G.D.W. and Waugh A.R., J. De Physique Supplement to No.12 45 (1984) 329.

[5] Miller M.K., Beaven P.A. and Smith G.D.W., Surface and Interface Analysis, 1 (1979) 149.

[6] Rose, D.J., J. Appl. Phys. 27 (1956) 215.

[7] Birdseye P.J., Smith D.A. and Smith G.D.W., J. Phys. D. (Appl. Phys.) 7 (1974) 1642.

[8] Worrall G.M., Private Communication.

[9] Davies D.M., D.Phil Thesis, Cambridge (1970).

[10] Davies D.M. and Ralph B., J.I.S.I., 210 (1972) 262.

[11] Irani J.J. and Honeycombe R.W.K., J.I.S.I. 203 (1965) 826.

[12] Morikawa M., Komatsu H. and Tanino M., J. Electron Microscopy, 22 (1973) 99.

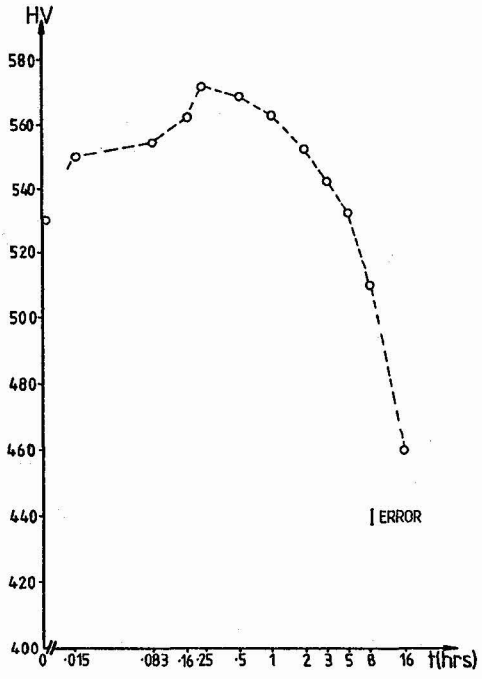

Fig.1 Vickers Hardness vs ageing time at 510°C (20kg load).

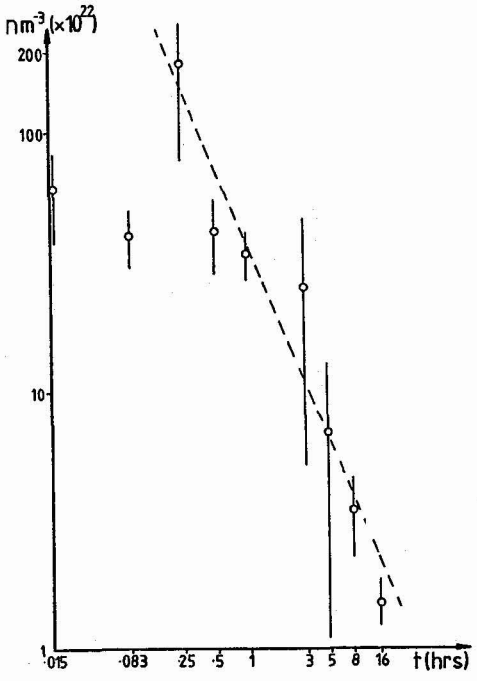

Fig.3 Particle number density vs ageing time.

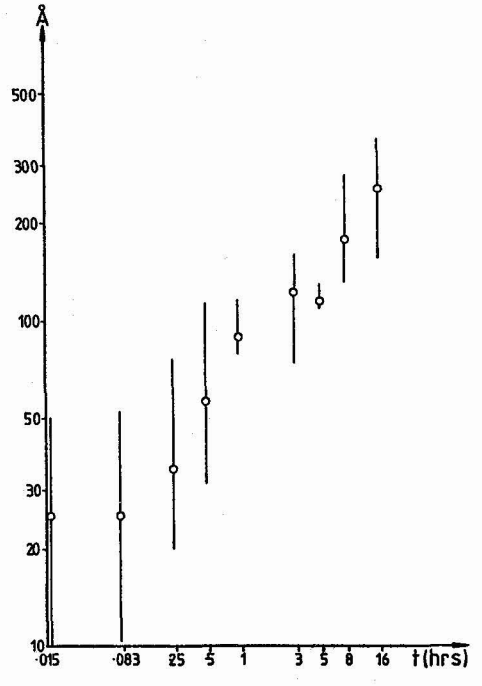

Fig.4 Apparent particle size vs ageing time.

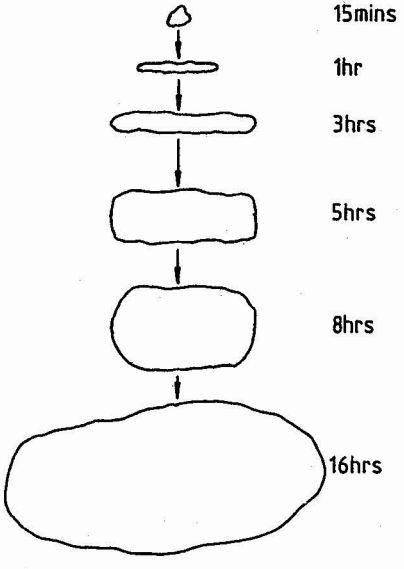

Fig.5 Evolution of particle morphology as a function of ageing time.

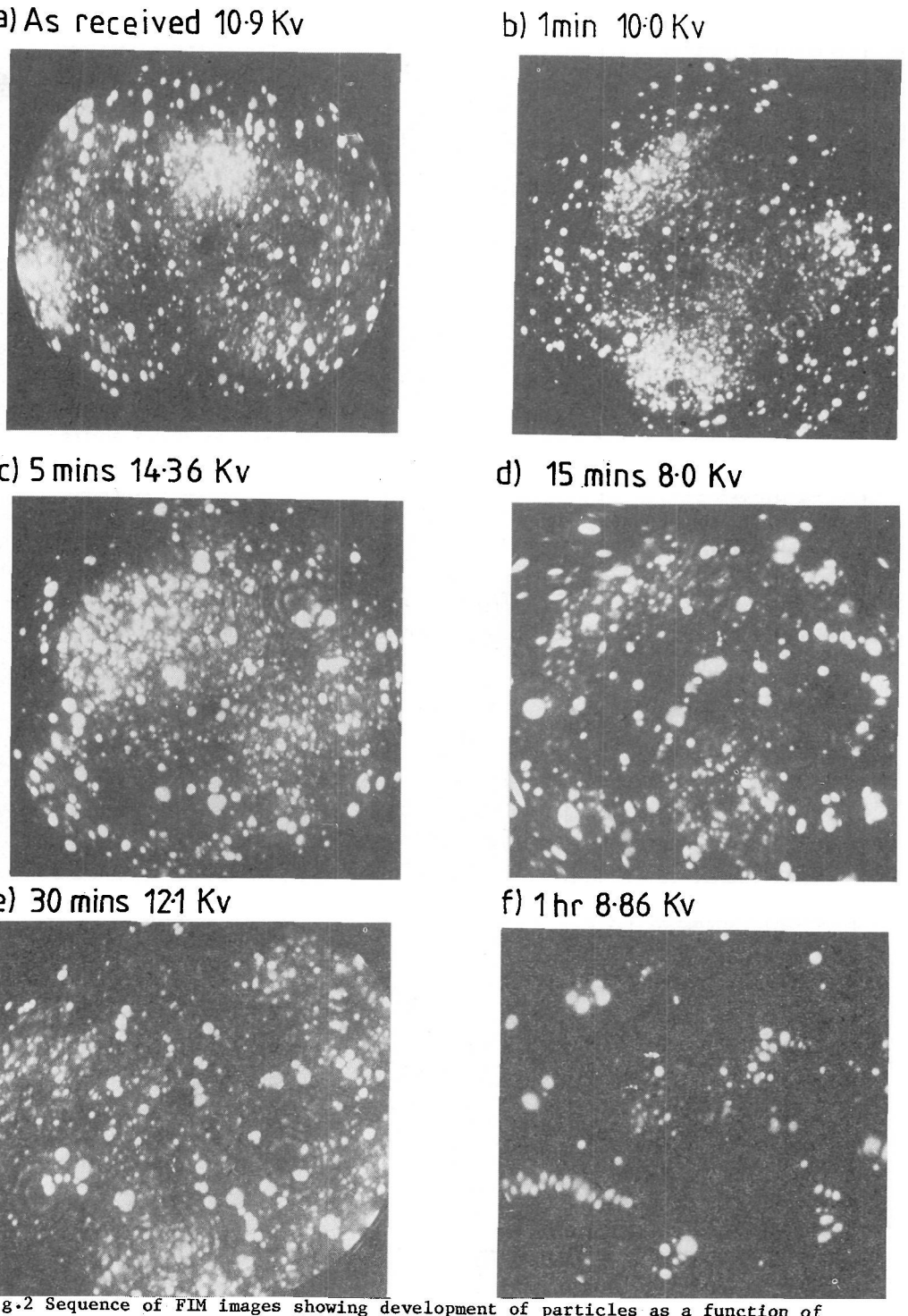

Fig.2 Sequence of FIM images showing development of particles as a function of ageing time at 510°C. All micrographs were recorded using neon image gas.

g) 3 hrs 7·5 Kv

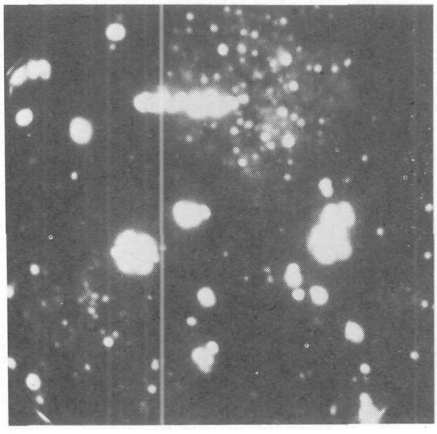

h) 3hrs 7·5 Kv

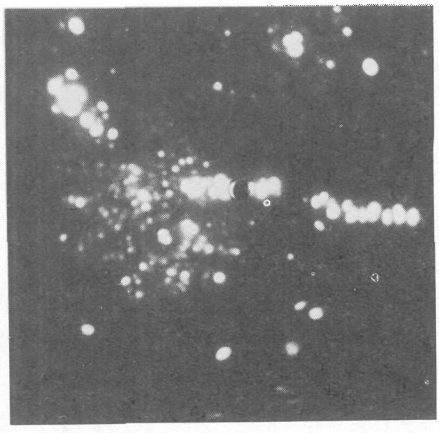

i) 5hrs 5·6 Kv

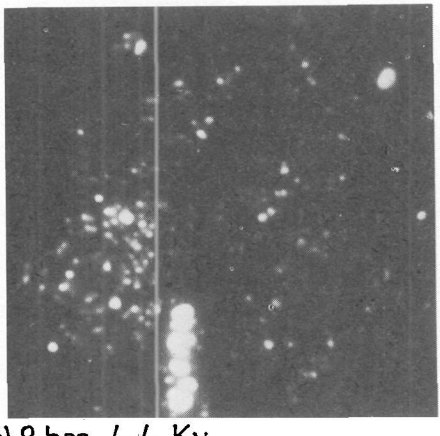

j) 5 hrs 8·15 Kv

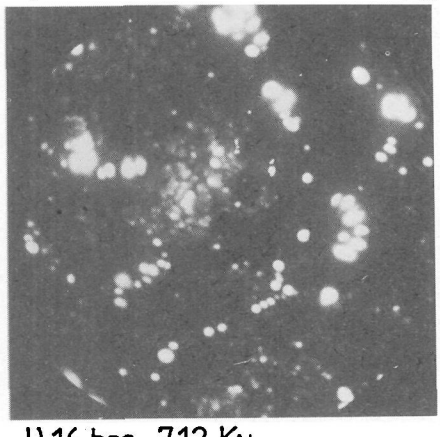

k) 8 hrs 4·4 Kv

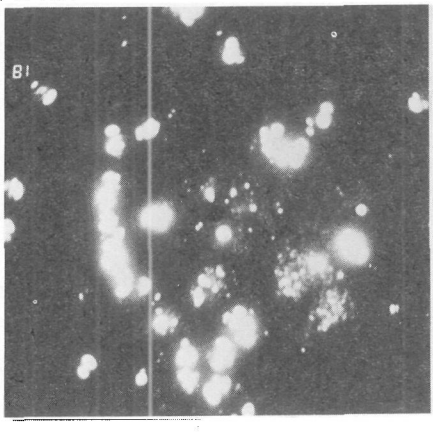

l) 16 hrs 7·12 Kv

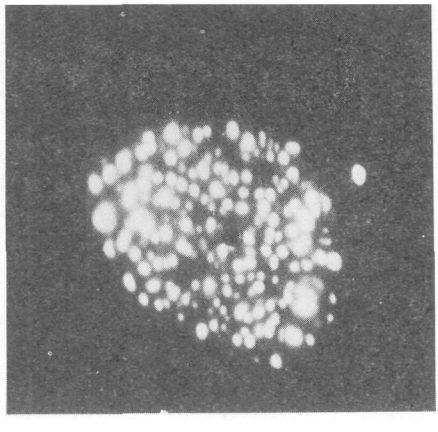

Fig.2 Continued.